Microvascularization of the Midbrain in Lylei's Flying Fox (*Pteropus lylei*)

Sirinush Sricharoenvej, Ph.D.*
Paowana Uthaichotiwan, D.V.M., M.Sc.**
Sanjai Sangvichian, M.D.*

Abstract : **Midbrain vascular casts of the Lylei's flying foxes (*Pteropus lylei*) were prepared by infusion of Batson's No. 17 plastic mixture into the blood vessels and examined by stereomicroscopy and scanning electron microscopy. Histological study of the midbrain was also performed. It was found that the midbrain of Lylei's flying fox was supplied by the branches of the vertebrobasilar system. These branches gave off the penetrating arteries, which coursed radially into the internal part of the midbrain toward the cerebral aqueduct. These arteries could be divided into anteromedial, anterolateral, posterolateral and posteromedial groups, according to the points of entry and supplying areas. The arteries ramified into arterioles and capillaries, respectively. The density of the capillary network in the midbrain was closely related to the density of the nerve cells in midbrain nuclei. Less vascularity was found in the areas occupied by nerve fibers. The arterial anastomoses could be observed on the surface of the midbrain. The venous drainage in the midbrain could be divided into three major groups according to the areas of drainage. Firstly, anterior or petrosal group drained the blood from the areas ventral to cerebral aqueduct into the superior petrosal sinus. Secondly, the superior or galenic group emptied the venous blood from the thalamocollicular and dorsal aqueductal veins into the great cerebral vein of Galen and rectus sinus, respectively. Thirdly, the posterior group collected blood from the collicular veins into the rectus sinus. Finally, both rectus and superior petrosal sinuses drained into the external jugular vein and partially into the internal jugular vein.**

Key words : Midbrain, Lylei's flying foxes, Microvascularization

เรื่องย่อ : **การศึกษาโครงหลอดเลือดโดยละเอียดของสมองส่วนกลางในค้างคาวแม่ไก่**

ศิรินุช ศรีเจริญเวช ปร.ด.*, ภาวนา อุทัยโชติวรรณ สพ.บ., วท.ม., สรรใจ แสงวิเชียร พ.บ.***

**ภาควิชากายวิภาคศาสตร์, คณะแพทยศาสตร์ศิริราชพยาบาล, มหาวิทยาลัยมหิดล, กรุงเทพมหานคร 10700. **ภาควิชากายวิภาคศาสตร์, คณะสัตวแพทยศาสตร์, จุฬาลงกรณ์มหาวิทยาลัย, กรุงเทพมหานคร 10330.*

สารศิริราช 2546; 55: 655-667.

การศึกษาโครงหลอดเลือดโดยละเอียดของสมองส่วนกลางในค้างคาวแม่ไก่ ด้วยเทคนิค vascular corrosion cast ภายใต้กล้องจุลทรรศน์อิเลคตรอนแบบส่องกราด ร่วมกับเทคนิคทางเนื้อเยื่อวิทยา พบว่าสมองส่วน

**Department of Anatomy, Faculty of Medicine Siriraj Hospital, Mahidol University, Bangkok 10700, Thailand.*
***Department of Anatomy, Faculty of Veterinary Medicine, Chulalongkorn University, Bangkok 10330, Thailand.*

กลางในค้างคาวแม่ไก่ ได้รับเลือดมาจากแขนงของ vertebrobasilar system ซึ่งจะให้แขนงแทงทะลุสมองส่วนกลางในแนวรัศมีพุ่งเข้าสู่ cerebral aqueduct หลอดเลือดที่เลี้ยงเนื้อเยื่อภายในสมองส่วนกลางสามารถแบ่งออกเป็น 4 กลุ่ม โดยอาศัยจุดที่หลอดเลือดแตกแขนงเข้าสู่ภายในและขอบเขตที่ส่งแขนงไปเลี้ยง ซึ่งได้แก่ anteromedial, anterolateral, posterolateral และ posteromedial หลอดเลือดแดงเหล่านี้จะแตกแขนงเป็นหลอดเลือดแดงขนาดเล็กๆ และค่อยๆ ลดขนาดลง จนในที่สุดจะให้เป็นร่างแหของหลอดเลือดฝอย ซึ่งหนาแน่นในบริเวณที่เป็นกลุ่มของเซลล์ประสาทของสมองส่วนกลางและมีความหนาแน่นน้อยในบริเวณที่เป็นเส้นใยประสาท ลักษณะของการเชื่อมติดต่อกันของหลอดเลือดแดงจะพบได้เฉพาะบริเวณผิวของสมองส่วนกลางเท่านั้น และพบว่าหลอดเลือดฝอยในสมองส่วนกลางเป็นชนิดไม่มีรูพรุนที่ผนังหลอดเลือด หลอดเลือดฝอยเหล่านี้จะรวมกันเป็นหลอดเลือดดำขนาดเล็กเพื่อนำเลือดออกจากสมอง ซึ่งแบ่งออกเป็น 3 กลุ่ม คือ กลุ่ม anterior หรือ petrosal, กลุ่ม superior หรือ galenic, และกลุ่ม posterior แล้วในที่สุดเลือดจะไหลเข้าสู่ external jugular vein เป็นส่วนใหญ่ และส่วนน้อยเข้าสู่ internal jugular vein

คำสำคัญ Midbrain, Lylei's flying foxes, Microvascularization

INTRODUCTION

Bats, classified in the order of Chiropter, are the only mammals that can fly like birds. Chiroptera can be divided into two suborders; the suborder Megachiroptera (fruit-bat) and the suborder Microchiroptera (insect-bat). The large fruit-bats found in Thailand are called Lylei's flying foxes (*Pteropus lylei*) (Figure 1). They have large eyes and small ears.[1-3] To locate places and obstacles, they use visual function, whereas the insect-bats use hearing function.[1,3-5] The midbrain or mesencephalon is a part of brain stem situated between the diencephalon and the pons. It contains many nuclei and fibers which have important functions in visual and hearing pathways.[6,7] Regarding the midbrain vascularity, it is nourished by branches from the arterial circle of Willis.[8,9] As the three-dimensional configuration of the midbrain vascular system is difficult to visualize by histological methods using light microscopy, it is of interest to employ vascular corrosion cast technique in conjunction with scanning electron microscopy (SEM) to elucidate the midbrain microvascularizaˉtion in Lylei's flying fox (*Pteropus lylei*).

MATERIALS AND METHODS

Fifteen adult Lylei's flying foxes (*Pteropus lylei*) of both sexes, weighing between 250-260 g, were used for this study. Under chloroform anesthesia, the thoracic cage of each animal was cut to expose the heart. Then 0.05 ml of heparin (Leo 5,000 iu/ml) was immediately injected into the left ventricle to prevent blood clotting. The left ventricle was cannulated with an 18G needle and the right atrium was then cut. The blood was washed out from the vessels by perfusion of 500-1,000 ml of 0.9% NaCl, via the canula. The injection of Batson's No. 17 plastic mixture and the preparation of midbrain vascular casts were carried out according to the methods previously described.[9-11] The midbrain vascular casts were cross-sectioned with razor blade under a stereomicroscope. Each cast was mounted on a metal stub and coated with carbon and gold/palladium before examining and photographing it under stereomicroscope and SEM at accelerating voltage of 15 kV.

In addition, the midbrain from animals without plastic injection were fixed in Bouin's fixative, dehydrated in a graded series of ethanol, sectioned at 7 μm thickness and stained with 1% Cresyl Violet for simultaneous visualization of the various areas in the midbrains.

RESULTS

The largest part of the brain stem in the Lylei's flying fox was midbrain. It could be divided

into three regions: tectum, tegmentum and crus cerebri. Tectum was dorsally covered by occipital poles of cerebral hemispheres and cerebellum (Figure 1). It contained superior and inferior colliculi. The superior colliculi were relatively larger than the inferior ones (Figures 2, 3). The superior collicular region was characterized by six laminated layers (strata) of nerve cells and fibers. This region could be subdivided into zonal layer, superficial gray layer, optic layer, intermediate gray and white layer, deep gray layer and deep white layer that was adjacent to the periaqueductal gray (Figure 9). There were multipolar cells within the various tectal layers. The second region of the midbrain was tegmentum, located between collicular eminences dorsally and the basal portion ventrally. This part of the midbrain was composed of many nuclei and fibers (Figures 7, 9). The crus cerebri situated on the ventral surface of the midbrain containing descending fibers of motor tracts from cerebral cortex (Figures 7, 9).

The study with vascular corrosion cast technique revealed that internal carotid and vertebrobasilar systems supplied the Lylei's flying fox brain. It was obvious that the blood supply of the midbrain in Lylei's flying fox was from the posterior communicating artery (PCoA) of the internal carotid artery (ICA) and branches of the vertebrobasilar system, namely the basilar artery (Ba), anterior cerebellar artery (ACe) and posterior cerebral artery (PCA) (Figures 4, 19). However, the branches from the PCA were the major sources (Figures 4, 19). These branches gave off the penetrating arteries, which coursed radially into the internal part of the midbrain toward the cerebral aqueduct. These arteries were divided into anteromedial, anterolateral, posterolateral and posteromedial groups, according to the points of entry and supplying areas (Figures 8, 10-12). The anteromedial group consisted of the paramedian branches which were the direct perforating branches of the basilar bifurcation, proximal segment of PCA (P1) and ACe (Figures 4, 8). The anterolateral group received from the ACe and penetrating branches of P1 segment of PCA (Figures 8, 12). The penetrating branches of the posterolateral or lateral group were the direct branches from the initial portion of the collicular and median posterior choroidal arteries (MPChA) (Figures 8, 10). The branches forming the posteromedial or posterior group came from the ACe, collicular arteries (ColA) of posterior portion of secondary portion of PCA (P2P) and MPChA (Figures 8, 10). It was noted that a characteristic of these penetrating branches was their centripetal direction (Figure 8).

In the anteromedial group, the paramedian branches entered the midbrain in a fanlike manner to supply the medial part of the midbrain. They distributed in the areas of interpeduncular fossa (IF), crus cerebri and tegmentum. Finally, they ended at the ventral part of the cerebral aqueduct. The oculomotor nuclear complex was supplied by the paramedian thalamomesencephalic branches. The right and left paramedian branches ran in the IF and penetrated the midbrain at right angle near the midline. They ran in parallel to each other in the dorsal direction to reach the floor of the cerebral aqueduct and also ran in curve, arcuate and passed laterally before entering the oculomotor nerve nuclear complex. They embroced the area corresponding to the medial side of the red nucleus and also supplied the nucleus of the troclear nerve, medial longitudinal fasciculus (MLF) and decussation of superior cerebellar peduncles. The collateral circulations among the arteriolar branches of the right and the left paramedian arteries were observed. Among the three parts of the midbrain, the tegmentum was the most vascularized area as it contained many nuclei or groups of neurons. The tectum, dorsal to the cerebral aqueduct, did not received the blood from arteries of this group but from the posterior group (Figures 4, 8, 11).

The anterolateral group consisted of the penetrating branches of ACe and P1 segment (Figures 4, 8). These penetrating branches supplied the crus cerebri, and some of them passed through the crus cerebri to supply the substantia nigra (SN), lateral sides of red nucleus, oculomotor and trochlear nerve nuclei. It was noted that the arteries of this group do not reach the cerebral aqueduct (Figures 4, 8, 11).

The posterolateral group was composed of the penetrating branches of the initial portions of the collicular and MPChA arteries that supplied the lateral part of the crus cerebri, lateral lemiscus and lateral part of the tegmentum (Figures 8, 12).

The posteromedial group was composed of the penetrating branches from the ACe, collicular artery of P2P and MPChA. The posteromedial group gave off branches to penetrate the colliculus (tectum) (Figures 8, 10). Many small arteries were seen piercing the surface of the colliculus and ended at various levels that related to the arrangement of the layers of superior colliculus (Figures 9, 10). The dense vascularization was seen in the superficial gray layer, intermediate gray and white layer, and deep gray layer.

Observing the vascular corrosion cast under SEM at high magnification, revealed the arterial anastomoses on the surface of the midbrain (Figure 17). After originating from the parent arteries on the surface of the midbrain, the arterial branches could be divided into two sets of penetrating arteries. The superficial set branched into arterioles and a capillary network in the superficial layer of the superior colliculus. The set of longer arteries went deeper and ramified into a capillary network in the deep and periaqueductal gray layers. It is evident that 3 to 4 microvascularization layers could be observed (Figures 10, 13, 14). After branching from the parent artery at the surface of the midbrain, the penetrating arteries rapidly reduced their diameters into arterioles and capillaries, respectively (Figures 13-17). The density of the capillary network in the midbrain was closely related to the density of the nerve cells in the midbrain nuclei. Less vascularity was found in the area occupied by nerve fibers (Figures 7-12). At higher magnification, there was no fenestration on the vascular cast of the capillary network (Figure 18).

The venous blood from the capillary network was collected into small venules (Figures 17-19). The small venules then drained into tributaries of veins and large veins on the surface of the midbrain. The venous blood from the tegmentum and crus cerebri (ventral part of cerebral aqueduct) drained into the collecting veins that were larger than the accompanying arteries (Figures 5, 15, 17). The collecting veins emptied the blood into the basal vein (BV) (Figures 5, 6, 19). The BV ended at the junction between the superior petrosal and transverse sinuses (Figures 5, 6, 19). It continued on the lateral side of the cerebral peduncle and bifurcated at the level caudal to the medial geniculate body before entering the superior petrosal sinus in the anterior or petrosal group.

The capillaries in the central part of the midbrain around the periaqueductal gray and the oculomotor nuclear complex collected the venous blood upward and dorsally into the lateral and dorsal aqueductal veins (Figures 17, 19). These joined with the thalamocollicular vein laying on the edge between the superior colliculus and thalamus. The thalamocollicular vein recieved the blood from the BV, which connected to the superior petrosal sinus and encircled the midbrain beneath the MPChA (Figures 5, 6, 19). The thalamocollicular vein drained into the great cerebral vein of Galen and the rectus sinus in superior and galenic group, respectively.

Small veins on the dorsal surface of the caudal part of superior colliculus drained the venous blood directly into transverse sinus. At the junction between the superior and inferior colliculi, there were two small veins running and joining each other at the midline before draining the blood into the dorsal aqueductal vein. After joining, they ran upward along the midline and connected to two or three veins of the colliculus at the caudal end of the quadrigeminal plate to form the collicular vein (Figures 5, 19). The collicular vein collected the venous blood from both colliculi into the rectus sinus in the posterior group. Finally, the venous blood from both rectus and superior petrosal sinuses drained mainly into the maxillary vein before entering the external jugular vein and partially into sigmoid sinus before entering the internal jugular vein (Figures 6, 19).

DISCUSSION

The midbrain of the Lylei's flying fox is relatively very large when compared with the whole brain stem. The dorsal surface of the midbrain is not visible from the dorsal aspect because it is covered mostly by the occipital pole of the cerebral hemispheres. This feature is common in all mammalian members of orders Marsupialia, Rodentia, Logomorpha and Primates.[12] The internal structure of the Lylei's flying fox midbrain can be divided into tectum, tegmentum and crus cerebri as in other mammals[13] as well as in man.[13-16] The tectum or roof consists of four prominences called corpora

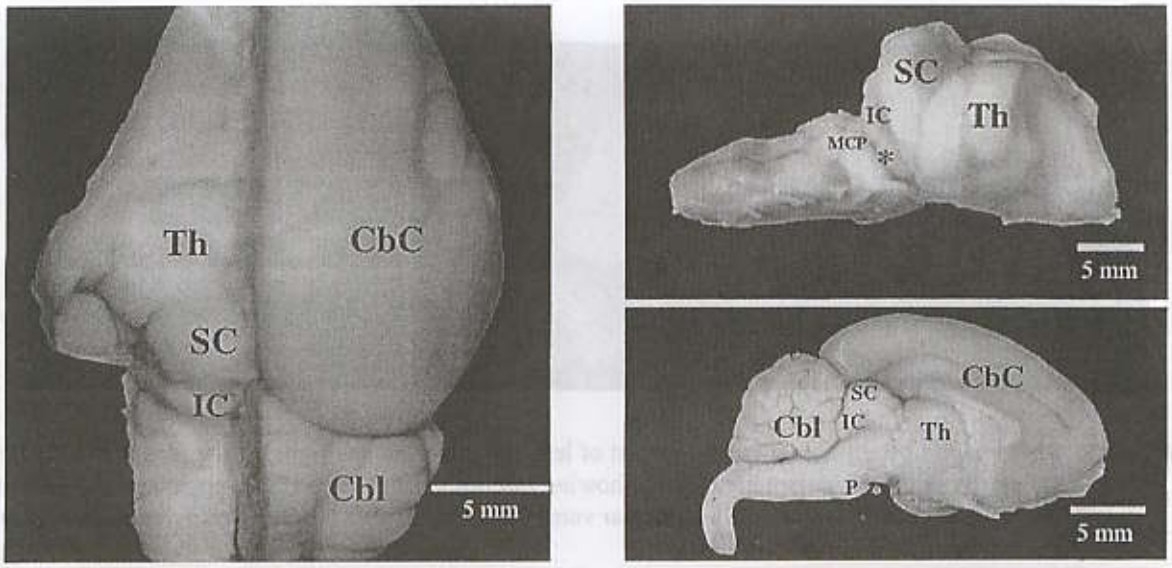

Figure 1. Photograph of the Lylei's flying fox brain, dorsal view, after removal of the left cerebral and cerebellar hemispheres, illustrating the dorsal aspect of the midbrain and related structures. Cerebral cortex (CbC), cerebellum (Cbl), thalamus (Th), superior colliculus (SC) and inferior colliculus (IC). Bar = 5 mm.

Figure 2. Photograph of the Lylei's flying fox brain, lateral view, after removal of both cerebral and cerebellar hemispheres, illustrating the lateral aspect of the midbrain and related structures. Superior colliculus (SC), inferior colliculus (IC), thalamus (Th) middle cerebellar peduncle (MCP) and medial geniculate body (*). Bar = 5 mm.

Figure 3. Photograph of the midsagittal section of the Lylei's flying fox brain, illustrating the midbrain and related structures. Cerebral cortex (CbC), cerebellum (Cbl), thalamus (Th), superior colliculus (SC), inferior colliculus (IC), pons (P) and interpeduncular fossa (*). Bar = 5 mm.

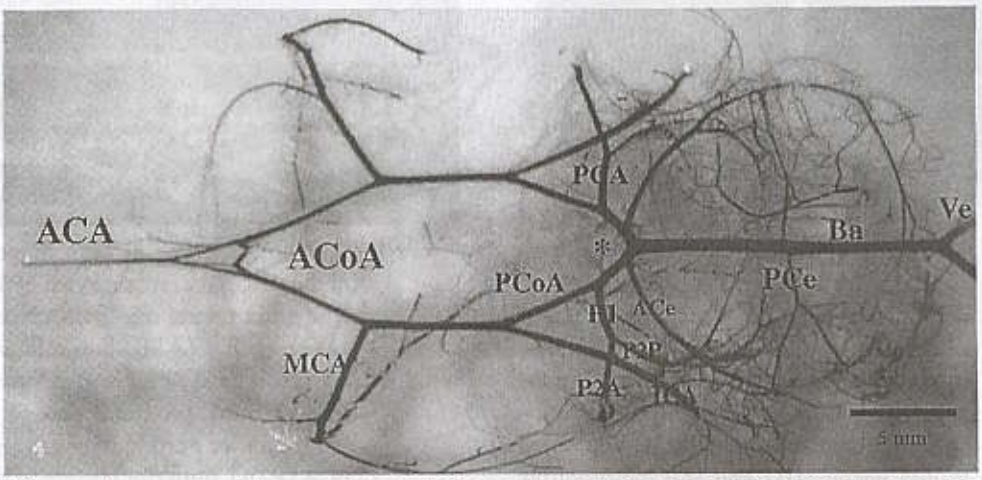

Figure 4. Stereomicrograph of the vascular corrosion cast, showing the main arterial supply of the Lylei's flying fox brain. Vertebral artery (Ve), basilar artery (Ba), basilar bifurcation (*), posterior cerebellar artery (PCe), internal carotid artery (ICA), anterior cerebellar artery (ACe), posterior cerebral artery (PCA), proximal part of the PCA (P1), anterior portion of secondary part of PCA (P2A), posterior portion of secondary part of PCA (P2P), posterior communicating artery (PCoA), anterior communicating artery (ACoA), middle cerebral artery (MCA), anterior cerebral artery (ACA). Bar = 5 mm.

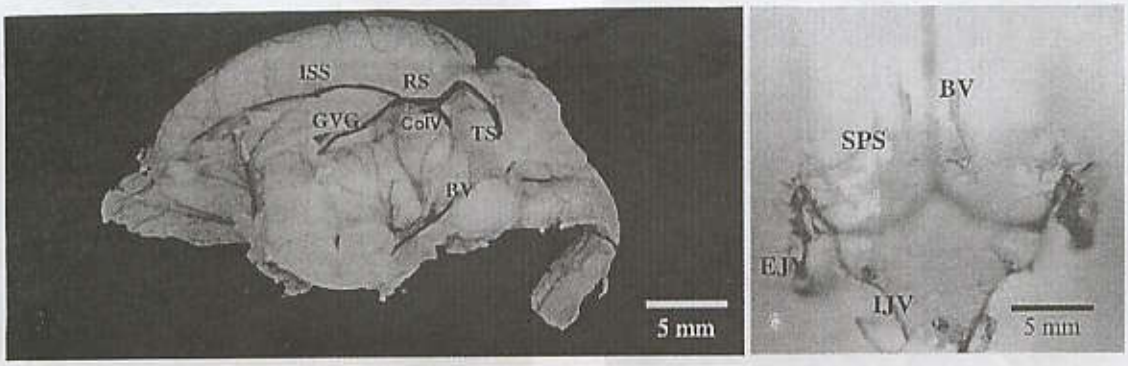

Figure 5. Photograph of the vascular corrosion cast of left half midbrain and right hemisphere in the Lylei's flying fox midbrain, dorsolateral view, showing inferior sagittal sinus (ISS), great cerebral vein of Galen (GVG), rectus sinus (RS), collicular vein (ColV), basal vein (BV) and transverse sinus (TS). Bar = 5 mm.

Figure 6. Photograph of the vascular corrosion cast of the venous drainage of midbrain in the Lylei's flying fox, dorsal view, showing basal vein (BV), superior petrosal sinus (SPS), external jugular vein (EJV) and internal jugular vein (IJV). Bar = 5 mm.

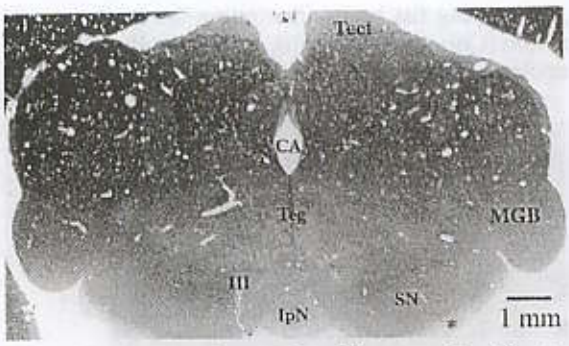

Figure 7. Stereomicrograph of the rostral midbrain in the Lylei's flying fox, cross section, demonstrating the three major regions and internal structures. Tectum (Tect), tegmentum (Teg), crus cerebri (*), substantia nigra (SN), medial geniculate body (MGB), cerebral aqueduct (CA), oculomotor nerve (III) and interpeduncular nucleus (IpN). Bar = 1 mm

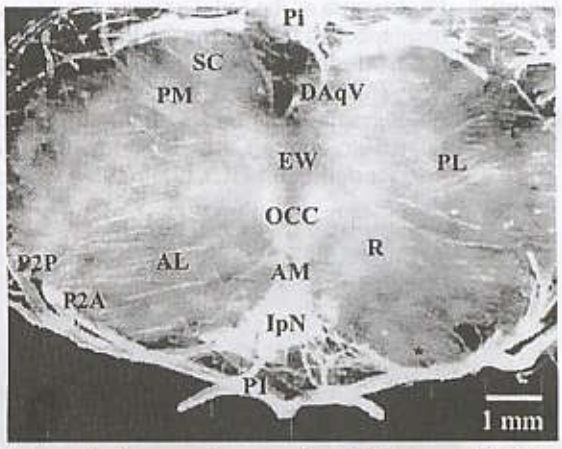

Figure 8. Stereomicrograph at high magnification of the vascular corrosion cast of the Lylei's flying fox rostral midbrain, cross section, anteromedial (AM), anterolateral (AL), posterolateral (PL) and posteromedial (PM) groups, proximal part of the PCA (P1), anterior portion of secondary part of PCA (P2A), posterior portion of secondary part of PCA (P2P), dorsal aqueductal vein (DAqV), superior colliculus (SC), oculomotor nuclear complex (OCC), Edinger-Westphal nucleus (EW), red nucleus (R), interpeduncular nucleus (IpN) and crus cerebri (*). Bar = 1 mm.

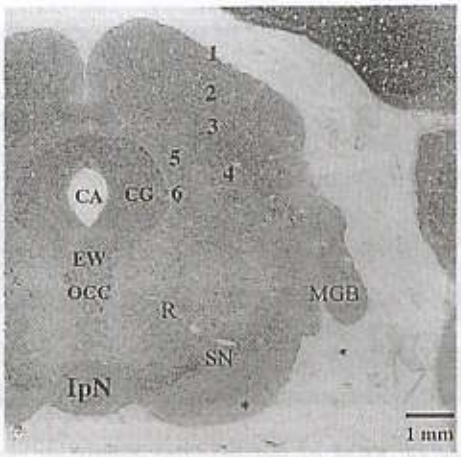

Figure 9. Stereomicrograph of the rostral midbrain in the Lylei's flying fox, cross section, demonstrating internal structures. Six layers of superior colliculus (1-6), crus cerebri (*), medial geniculate body (MGB), substantia nigra (SN), cerebral aqueduct (CA), periaqueductal gray (CG), oculomotor nuclear complex (OCC), Edinger-Westphal nucleus (EW), red nucleus (R), and interpeduncular nucleus (IpN). Bar = 1 mm.

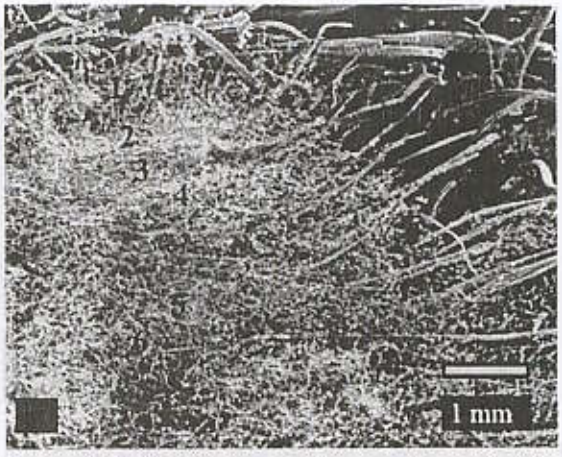

Figure 10. SEM of the vascular corrosion cast of the midbrain in the Lylei's flying fox, showing the six layers of left superior colliculus. Zonal layer (1), superficial gray layer (2), optic layer (3), intermediate gray and white layer (4), deep gray layer (5) and deep white layer (6). Bar = 1,000 μm.

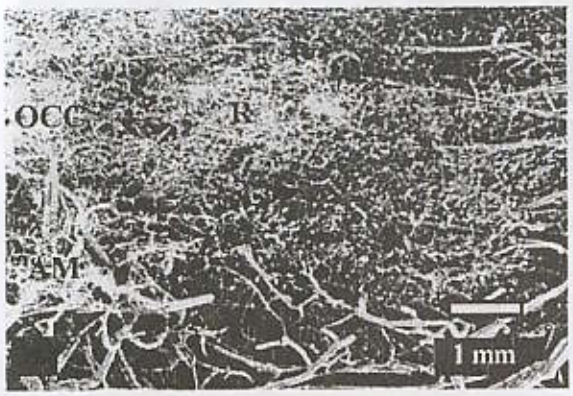

Figure 11. SEM of the vascular corrosion cast of the midbrain in the Lylei's flying fox, showing the left tegmentum of superior colliculus, anteromedian group (AM), oculomotor nuclear complex (OCC), red nucleus (R). Bar = 1,000 μm.

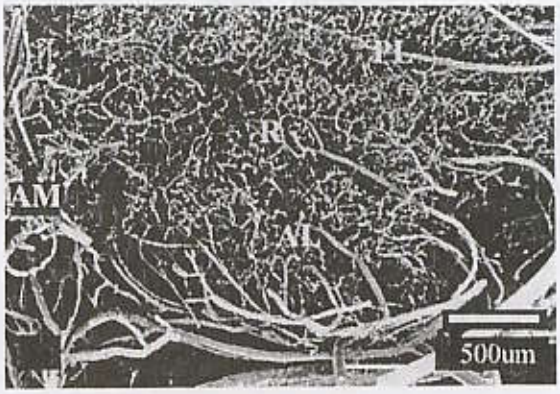

Figure 12. SEM of the vascular corrosion cast of the midbrain in the Lylei's flying fox, showing the anteromedial (AM), anterolateral (AL), posterolateral (PL) groups, red nucleus (R). Bar = 500 μm.

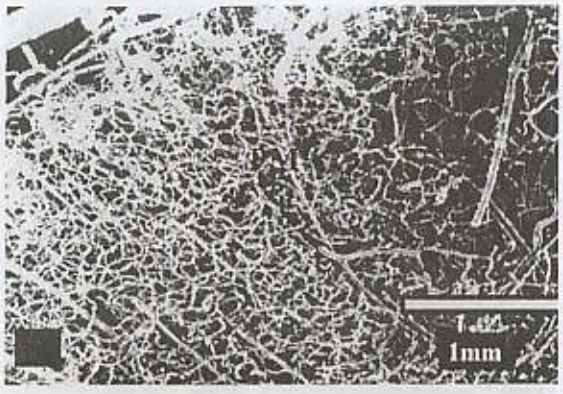

Figure 13. SEM of the vascular corrosion cast of the midbrain in the Lylei's flying fox, showing the posteromedial group (PM). Bar = 1,000 μm.

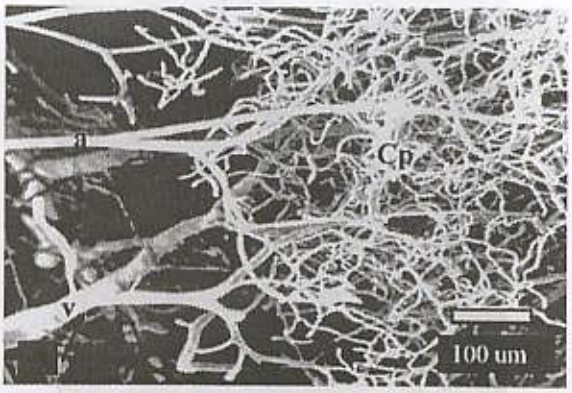

Figure 14. SEM of the vascular corrosion casts of the midbrain of the Lylei's flying fox showing the arterioles (a), venules (v) and capillary plexus (Cp) in anterolateral group. Bar = 50 μm.

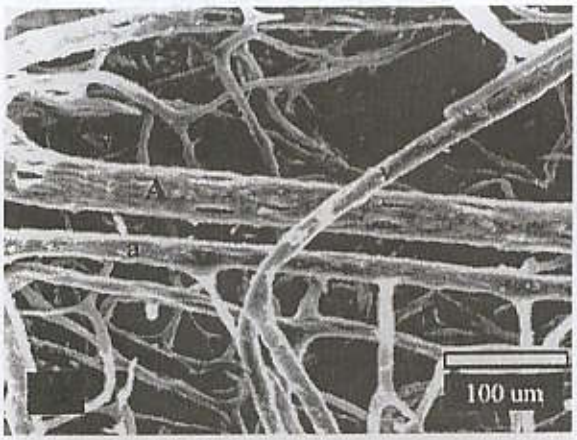

Figure 15. SEM of the vascular corrosion cast of the Lylei's flying fox midbrain, high magnification showing artery (A), arterioles (a), venules (v). Bar = 100 μm.

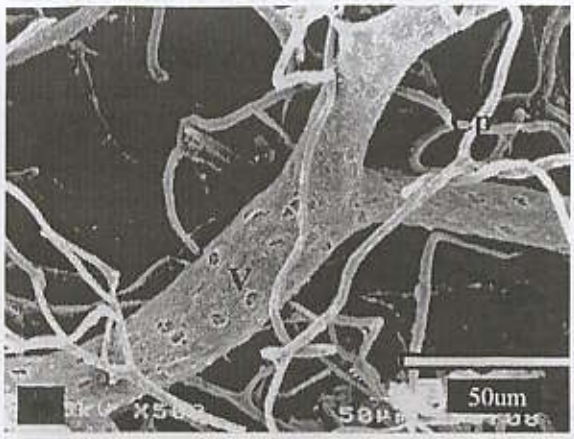

Figure 16. SEM of the vascular corrosion cast of the Lylei's flying fox midbrain, dorsal aqueductal vein (V), capillary plexus (Cp). Bar = 50 μm.

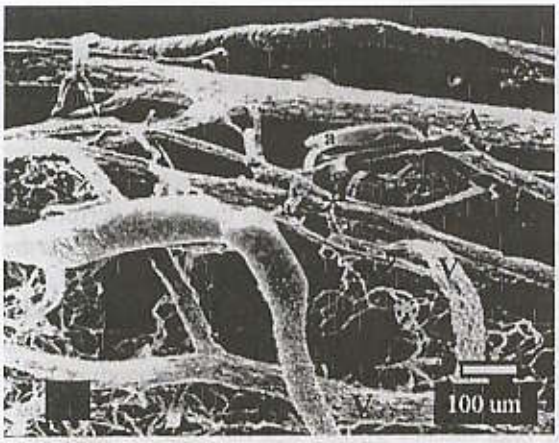

Figure 17. SEM of the vascular corrosion cast of the midbrain in the Lylei's flying fox, showing the anastomosis of collicular surface (*) between arteriole (a), artery (A), and venule (v). Bar = 100 μm.

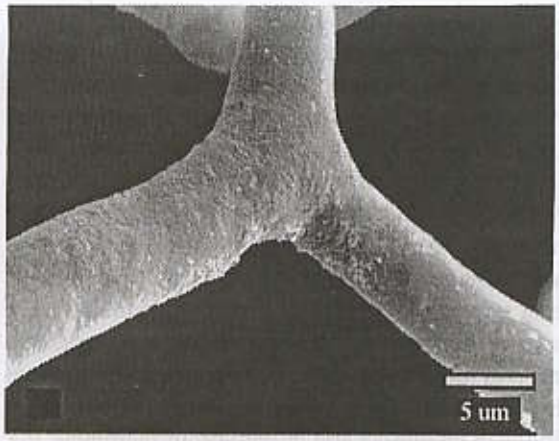

Figure 18. SEM of the vascular corrosion cast of the non-fenestrated capillary of the Lylei's flying fox midbrain. Bar = 5 μm.

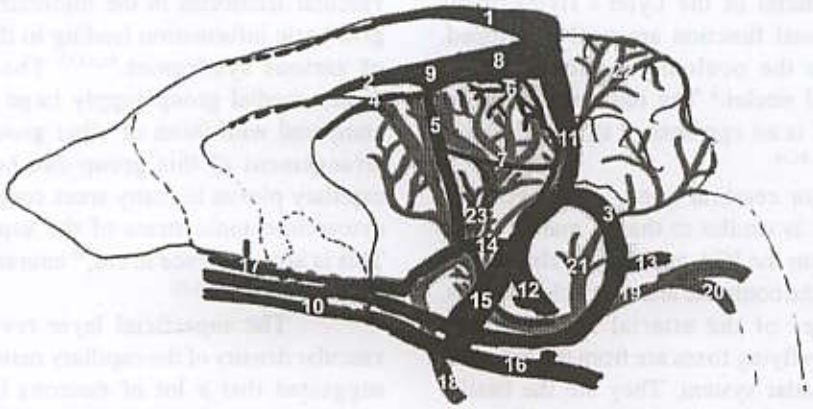

Figure 19. Diagram of the Lylei's flying fox brain, illustrating the arterial supply and the venous drainage of the midbrain. 1. Superior sagittal sinus 2. Inferior sagittal sinus 3. Sigmoid sinus 4. Internal cerebral vein 5. Thalamocollicular vein 6. Collicular vein 7. Dorsal aqueductal vein 8. Rectus sinus 9. Great vein of Galen 10. Cavernous sinus 11. Transverse sinus 12. Maxillary vein 13. Internal jugular vein 14. Basal vein 15. Superior petrosal vein 16. Inferior petrosal vein 17. Middle cerebral vein 18. Internal carotid artery 19. Basilar artery 20. Vertebral artery 21. Posterior cerebellar artery 22. Anterior cerebellar artery 23. Posterior cerebral artery.

quadrigemina. The larger superior colliculus continues into the diencephalons on its upper end. The smaller inferior colliculus connects to the pons at its lower border. The superior colliculus in the Lylei's flying fox is remarkably large and well developed with distinctively differentiated layers, the same as in common tree shrew.[18-20] Among mammals, the best development with very distinct layers can be observed in Lylei's flying foxes as well as in gray squirrels,[21] rat,[11] and cat.[22] Some animals have a common rapid locomotive behavior and arboreal niche such as flying lemur, squirrel and tree shrew, therefore their superior colliculus is very large. Unlike in prosimian and insectivorous mammals, the superior colliculus is relatively small and less differentiated. The well-developed superior colliculus in the Lylei's flying fox indicates the correlated functions of the eyes more than that of the ears. This evidence is an important criteria in the classification of Chiroptera. It is indicated that this kind of bats does not depend entirely upon the hearing sensation, but that its flight requires a good sense of vision to locate the places and obstacles ahead.[1,2] The tegmental nuclei of the Lylei's flying foxes related to the visual function are well developed. These nuclei are the oculomotor, trochlear and Edinger-Westphal nuclei.[8] The red nucleus in the Lylei's flying fox is an egg-shaped structure like in other mammals.[13,23,24]

The major cerebral artery of the brain in Lylei's flying fox is similar to that in man.[25] These branches arise from the ICA and the vertebrobasilar system that form the complete arterial circle of Willis. The main sources of the arterial supply to the midbrain in Lylei's flying foxes are from the branches of the vertebrobasilar system. They are the basilar bifurcation, superior cerebellar, PCA, MPChA and ColA similar to those of man,[6,7,26,27] guinea pig,[28,29] dog[30,31] and common tree shrew.[9] The midbrain of the submammalian vertebrates such as fishes, amphibians, reptiles and birds are supplied by branches from the caudal division of the ICA[8]. In higher mammals,[28-31,36,37] man,[39,40] common tree shrew[9] as well as in the Lylei's flying foxes, the PCA is the major source of blood supply to the midbrain. This artery in the rat[32] and man[41-44] usually originates from the Ba. In the human embryo, the PCA arises as a branch of ICA.[27,45,46].

The PCA in Lylei's flying foxes can be divided into four segments as in common tree shrew and man.[42,43,47] The P1 segment of the PCA, or mesencephalic artery, is the segment that is situated between the proximal portion of the PCA extending from the basilar bifurcation to PCoA.[27,41-45,48-50] The P1 segment of the PCA gives the direct perforating arteries in the interpeduncular fossa and supplies the midline region. Then, they send the short and long branches to encircle the midbrain and give the smaller branches to penetrate the midbrain at right angle into the tissues and reach the cerebral aqueduct. The penetrating arteries exhibit a radial pattern as appears in man,[41,45,51,52] guinea pig,[28,29] dog,[30,31] anuran,[53] common tree shrew[9] and submammalian vertebrates.[8] The general radial pattern of the internal vascularity as seen in the midline of the Lylei's flying foxes can be observed in all vertebrates including primates.

The arterial supply of the Lylei's flying fox midbrain is divided into anteromedial, anterolateral, posterolateral and posteromedial groups according to their points of penetration and the territories that they supply. The origins of the arteries and the arterial vascular territories in the midbrain and brain stem give basic information leading to the understanding of various syndromes.[52,54,55] The arteries of the posteromedial group supply large territories when compared with those of other groups. The internal arrangement of this group can be observed as a capillary plexus in many areas corresponding to the cytoarchitectonic strata of the superior colliculus. This is also evidence in cat,[56] anuran,[53] common tree shrew[9] and man.[41,52]

The superficial layer reveals the highest vascular density of the capillary networks. It has been suggested that a lot of neurons in this layer are associated with visual activities.[18,19,57,58] It is evident that there is a close relationship among cytoarchitecture, richness of the capillary networks, and the neuronal activity. The penetrating arterioles terminate into capillary networks as observed in all mammals, especially in the primates. In opossums and marsupials, however, the capillary networks are not present, and capillary loops are found instead[34,59]. In addition, the capillaries in the midbrain of the Lylei's flying foxes are without fenestration. Fenestrated capillaries have been reported in the early-developed chicken optic tectum.[60]

With the light microscopic study of the midbrain paraffin sections in parallel with those of the midbrain vascular cast sections, it was obvious that the midbrain nuclei of the Lylei's flying fox, located in the tegmentum, had a large blood supply. This finding is also true in common tree shrew,[9] dog[30] and guinea pig.[29] Dense vascularity could also be seen in the oculomotor nuclear complex, red nucleus, trochlear nucleus and interpeduncular nuclei. The less vascularized areas were the crus cerebri and lateral part of the midbrain. These areas contained predominantly nerve fibers. It is quite certain that the degree of vascularity depends on the density of nerve cells.

The venous drainage of the midbrain in the Lylei's flying fox is quite similar to that in common tree shrew[9] and man[41,61-65] but somewhat different from the guinea pig[29] and dog.[13,30] In man and in the common tree shrew, the venous drainage in the midbrain can be divided into anterior or petrosal, superior or galenic and posterior groups[66,67] as in the midbrain of the Lylei's flying foxes. It is noted that the basal vein in the Lylei's flying foxes drains the venous blood into both petrosal and galenic groups but predominantly into the great cerebral vein of Galen as in the common tree shrew[9] and man.[62,64,66,67] However, in the dog, this vein drains mainly into the superior petrosal sinus.[69] The collicular or quadrigeminal veins of the Lylei's flying foxes drain the venous blood into the rectus sinus as in the common tree shrew, but in man this vein flows into the great vein of Galen.[9,64,71]

The Lylei's flying fox (*Pteropus lylei*) has been classified as a member of the suborder Megachiroptera (fruit-bat) in the order Chiroptera.[1,2] In this study it is obvious that the superior colliculus of the Lylei's flying fox is more well-developed than the inferior colliculus. Furthermore, the density of blood supply in the area of the superior colliculus is higher than in the area of the inferior colliculus. These results indicate that this bat uses visual function to locate the place and obstacle ahead more than hearing function, whereas Microchiroptera (insect-bat) uses echolocation for prey.[1-3] This characteristic is used as a criteria in the classification of Chiroptera, which can be divided into two suborders; the suborder Megachiroptera (fruit-bat) and the suborder Microchiroptera (insect-bat).

CONCLUSIONS

The vertebrobasilar system and its branches are the major arterial supply of the midbrain in Lylei's flying foxes. These arteries can be classified as anteromedial, anterolateral, posterolateral, and posteromedial groups. Then, these vessels give off arterioles and capillaries to supply the internal structures. Moreover, the density of the capillary plexus is extremely corresponded to the numbers of nerve cells in the midbrain nuclei. No fenestration is observed on the vascular cast of the capillary. The venous blood drains into venules and veins, which are divided into three major groups: anterior or petrosal, superior or galenic, and posterior groups. These veins empty into great cerebral vein of Galen, superior petrosal and rectus sinus, which are communicated to external and internal jugular veins.

REFERENCES

1. Fenton MB. Bats. Revised ed. Checkmark Books, 2001.
2. Lekakul B, Maneely J. Mammals of Thailand. Kurusapa, Ladprao Press, Bangkok, 1977.
3. Parker S. Mammal. Dorling Kindersley Limited, London, 1989.
4. Boonneung J. The biology of Lylei's flying fox. [M. Sc. Thesis in Biology]. Bangkok: Faculty of Graduate Studies, Kasetsart University; 1975.
5. Chamhnoonthod T. General morphology and some certain microscopic structures of the central nervous system of the Lylei's flying fox. [M. Sc. Thesis in Anatomy]. Bangkok: Faculty of Graduate Studies, Mahidol University; 1979.
6. Bogousslavsky J, Maeder P, Regli F, Meuli R. Pure midbrain infarction: Clinical syndrome, MRI, and etiologic patterns. Neurology 1994; **44:** 2032-40.
7. Bulter AB, Hodos W. Comparative vertebrate neuroanatomy: evolution and adaptation. New York: Wiley-Liss; 1996.
8. Gillilan LA. A comparative study of the extrinsic and intrinsic arterial blood supply to brains of submammalian vertebrates. J Comp Neurol 1967; **130:** 175-96.

9. Duangchan C. Microvascularization of the midbrain in common tree shrew (*Tupaia glis*). [M. Sc. Thesis in Anatomy]. Bangkok: Faculty of Graduate Studies, Mahidol University; 2000.
10. Bamroongwong S, Somana R, Chunhabundit P, Rattanachaikunsopon P. Scanning electron microscopic study of the splenic vascular casts in common tree shrew (*Tupaia glis*). Anat Embryo 1991; **184:** 301-4.
11. Chunhabundit P, Somana R. Modification of plastic mixture for vascular corrosion cast to withstand electron beam at high magnification under SEM. Proc 4th Asia-Pacific Conference and Workshop on Electron Microscope. Bangkok, Thailand, 1988: 411-12.
12. Campbell CBG. The relationships of the tree shrew: The evidence of the nervous system. Evolution 1966; **20:** 276-81.
13. Crosby EC, Woodburne RT. The mammalian midbrain and isthmus region: The nuclear pattern of the non-tectal portions of the midbrain and isthmus in primates. J Comp Neurol 1943c; **78:** 441-82.
14. Williams PL, Wawick R, Dyson M, Braunister LH. Gray's Anatomy. 37th ed. New York: Churchill Livingstone; 1989.
15. Romanes GJ. Cunningham's manual of practical anatomy. Vol III: Head and neck and brain. 15th ed. New York: Oxford Medical Publications; 1993.
16. Kahle W, Leonardt H, Platzes W. Color atlas and text of human anatomy. Vol. III: Nervous system and sensory organ. 4th revised ed. New York: Theme Medical Publishers; 1993.
17. Moore KL, Persaud TVN. The developing human: Clinically oriented embryology. 5th ed. Philadelphia: W. B. Saunders Company; 1993.
18. Harting JK, Hall WC, Diamond IT, Martin GF. Anterograde degeneration study of the superior colliculus in *Tupaia glis*: Evidence for a subdivision between superficial and deep layers. J Comp Neurol 1973b; **138:** 361-86.
19. Casagrande VA, Harting JK, Hall WC, Damond IT, Martin GF. Superior colliculus of the tree shrew (*Tupaia glis*): Evidence for a structural and functional subdivision into superficial and deep layers. Science 1972; **177:** 444-47.
20. Casagrande VA, Diamond IT. Ablation study of the superior colliculus in the tree shrew (*Tupaia glis*). J Comp Neurol 1974; **156:** 207-38.
21. Robson JA, Hall WC. Projection from the superior colliculus to the dorsal lateral geniculate nucleus of the gray squirrel (*Sciurus carolinensis*). Brain Res 1967; **113:** 379-85.
22. Kawamura S, Sprague JM, Niimi K. Corticofugal projections from the visual cortices to the thalamus, pretectal and superior colliculus in the cat. J Comp Neurol 1976; **166:** 303-40.
23. Carpenter MB. A study of the red nucleus in rhesus monkey. J Comp Neurol 1956; **105:** 195-250.
24. Otabe JS, Horowitz A. Morphology and cytoarchitecture of the red nucleus of the domestic pig (*Sus scrofa*). J Comp Neurol 1970; **138:** 373-90.
25. Kimmaktong W. Hypothalamic vascularization in common tree shrew (*Tupaia glis*) as revealed by vascular corrosion cast/SEM technique. [M.S.Thesis in Anatomy]. Bangkok: Faculty of Graduate Studies, Mahidol University; 1998.
26. Pullicino PM. The course and territories of cerebral small arteries. In: Pullicino PM, Caplan LR, Hommed M, eds. Advance in Neurology. Vol. 62. New York: Raven Press; 1993 : 11-39.
27. Kaplan HA, Ford DH. The brain vascular system. Amsterdam: Elsevier; 1966.
28. Majewska-Michalska E. Vascularization of the brain in guinea pig. II. Regions of vascular supply and spatial topography of arteries in the particular parts of the brain. Folia Morphol (Warsz) 1995; **54:** 33-40.
29. Majewska-Michalska E. Vascularization of the brain in guinea pig. IV. Angioarchitectonics of the tectum, tegmentum and crura mesencephali. Folia Morphol (Warsz) 1997; **56:** 47-53.
30. Majewska-Michalska E. Blood supply of the tegmentum mesencephali in dog. Folia Morphol (Warsz) 1984; **43:** 35-41.
31. Majewska-Michalska E. Vascular architecture of the crus cerebri in dog. Folia Morphol (Warsz) 1986; **45:** 151-57.
32. Lee RM. Morphology of cerebral arteries. Pharmacol Ther 1995; **66:** 139-73.
33. Alpers BJ, Berry GR, Paddison RM. Anatomical studies of the circle of Willis in normal brain. Arch Neurol Psychiat 1959; **81:** 409-18.
34. Gillilan LA. Blood supply to primitive mammalian brains. J Comp Neurol 1972; **45:** 209-22.
35. Lake AR, Van Niekerk IJM, Le Roux CGJ, Trevor-Jones TR, Dewet PD. Angiology of the brain of the baboon *Papio ursinus*, the vervet monkey *Cercopithecus py gerithrus*, and the bush baby *Galago senegalensis*. Am J Anat 1990; **187:** 277-87.
36. Kanan CV. The cerebral arteries of *Camelus dronedarius*. Acta Anat (Basel) 1970; **77:** 605-16.
37. Gillilan LA. Extra- and intra-cerebral blood supply to brains of dog and cat. Am J Anat 1976; **136:** 237-54.
38. Anderson WD, Kubicek W. The vertebral-basilar system of the dog and relative to man and other mammals. Am J Anat 1971; **132:** 179-88.

39. Shoutz C, Dujovny M, Ausman JI, Diaz FG, Pearce JE, Berman SK, et al. Surgical anatomy of the arteries of the posterior fossa. J Neurosurg 1986; **64:** 540-44.
40. Kaplan H, Rebiner AM, Browder J. Anatomical study of the arteries of the midbrain, pons and medulla. Trans Am Neurol Assoc 1953; **78:** 54-56.
41. Stephens RB, Stilwell DL. Arteries and veins of the human brain. Springfield: Charles C Thomas; 1969.
42. Zeal AA, Rhoton AL. Microsurgical anatomy of the posterior cerebral artery. J Neurosurg 1979; **48:** 534-59.
43. Saeki N, Rhoton AL. Microsurgical anatomy of the upper basilar artery and the posterior circle of Willis. J Neurosurg 1977; **46:** 563-78.
44. Williams DJ. Origin of the posterior cerebral artery. Brain 1939; **509:** 175-80.
45. Kaplan HA. Arteries of the brain: An anatomic study. Acta Radiol 1956; **46:** 364-70.
46. Hassler O. Arterial pattern of human brainstem. Normal appearance and deformation in expanding supratentorial conditions. Neurology 1967; **17:** 368-75.
47. Milisavljevic M, Marinkovic S, Malobabic S. Anatomic basis for surgical approach to the distal segment of posterior cerebral artery. Surg Radiol Anat 1988; **10:** 159-66.
48. Segarra JM. Cerebral vascular disease and behavior. I. The syndrome of the mesencephalic artery (basilar artery bifurcation). Arch Neurol 1970; **22:** 408-18.
49. Hochman MS, Sowers JJ, Bruce-Gregories J. Syndrome of the mesencephalic artery: Report of a case with CT and necropsy findings. J Neurol Neurosurg Psychiatry 1985; **48:** 1179-81.
50. Percheron G. Arteries of the human thalamus. II. Arteries and paramedian thalamic territory of the communicating basilar artery. Rev Neurol (Paris) 1976; **132:** 309-24.
51. Foix CH, Hillemand P. Les arters de laxe encephalique jusquau diencephalon inclusivement. Rev Neurol (Paris) 1925a; **32:** 705-39.
52. Gillilan LA. The correlation of the blood supply to the human brainstem with clinical brainstem lesions. J Neuropathol Exp Neurol 1964; **23:** 78-108.
53. Lametschwandtner A, Albrecht U, Adam H. The vascularization of the anuran brain. The mesencephalon. A SEM study of vascular corrosion casts. Acta Zool (Stockh) 1978; **60:** 89-92.
54. Savioardo M, Bracchi M, Passerini A, Visciani A. The vascular tributaries in the cerebellum and brainstem: CT and MR study. AM J Neuroradiol 1987; **8:** 199-209.
55. Tatu L, Monlin T, Bogousslavsky J, Duvernoy H. Arterial territories of human brain: Brainstem and cerebellum. Neurology 1996; **47:** 1125-135.
56. Boiaekina IV. Neurono-vascular relations in the superior colliculus of the cat tectum mesencephali. Arkh Anat Gistol Embriol [Online] 1982; **83:** 34-7. Abstract from: NCBI Pubmed medline query: Unique Identifier 83099885.
57. Albano JE, Humphrey AL, Norton TT. Laminar organization of the receptive- field properties in tree shrew superior colliculus. J Neurophysiol 1978; **41:** 1130-54.
58. Albano JE, Norton TT, Hall WC. Laminar origin of the projections from the superficial layers of the superior colliculus in the tree shrew, *Tupaia glis*. Brain Res 1979; **173:** 1-11.
59. Wislocki GB. The unusual mode of development of the blood vessels of opossum's brain. Anat Rec 1939; **74:** 409-27.
60. Bertossi M, Mancini L, Favia A, Nico B, Ribotti D, Virgintino D, et al. Permeability-related structures in developing and mature microvessels of the chicken optic tectum. Bio Struct Morphog 1992; **4:** 134-52.
61. Holdorff H, Bradac GB. Intraparenchymatous pontomesencephalic vein: A radio-anatomical study. Acta Anat (Basel) 1974; **89:** 333-44.
62. Hassler O. Deep cerebral venous system in man: A microangiographic study on its areas of drainage and its anastomoses within the superficial cerebral veins. Neurology 1966; **16:** 505-11.
63. Ono M, Rhoton AL, Peace D, Rodriquez RJ. Microsurgical anatomy of the deep venous system of the brain. Neurosurgery 1984; **15:** 621-57.
64. Matsushima T, Rhoton AL, De Oliveira E, Peace D. Microsurgical anatomy of the veins of the posterior fossa. J Neurosurg 1983; **59:** 63-105.
65. Andeweg J. Consequences of the anatomy of deep venous outflow from the brain. Neuroradiology 1999; **41:** 233-41.
66. Huang YP, Wolf BS. The veins of the posterior fossa-Superior or galenic draining group. AJR 1965; **95:** 808-21.
67. Huang YP, Wolf BS, Antin SP. The veins of the posterior fossa-Anterior or posterior draining group. AJR 1968; **104:** 36-56.
68. Amstrong LD, Horowitz A. The brain venous system of the dog. Am J Anat 1971; **132:** 470-90.
69. Tamaki N, Taomoto K, Fujiwara K, Matsumoto S, Takeda H. The venous drainage of the tectum mesencephali. An anatomical angiographic study of the quadrigeminal veins. Neuroradiology 1976; **11:** 151-57.